1 Localization of light in three-dimensional disordered dielectrics

MARIAN RUSEK[†], and ARKADIUSZ ORŁOWSKI
Instytut Fizyki, Polska Akademia Nauk, Aleja Lotników 32/46, 02–668 Warszawa, Poland

1.1 INTRODUCTION

Investigations of the electron transport in disordered solids, usually semiconductors, led to the concept of localization of the electron wave functions. This phenomenon, known now as the Anderson localization, became a prominent part of contemporary condensed matter physics and it is still a vivid subject of theoretical and experimental research. As shown by Anderson [1], in a sufficiently disordered infinite material an entire *band* of electronic states can be spatially localized. In fact, the Anderson localization may be viewed as a transition from particle-like behavior described by the diffusion equation to wave-like behavior, which results in localization by interference. Indeed, the most plausible explanation of the Anderson localization is based on the interference effects in multiple elastic scattering of electrons on the material impurities [2].

As interference is the common property of all wave phenomena, the quest for some analogs of electron localization for other types of waves has been undertaken and many generalizations of electron localization exist, especially in the realm of electromagnetic waves [3, 4, 5, 6]. So-called weak localization of electromagnetic waves manifesting itself as enhanced coherent backscattering is presently relatively well understood theoretically [7, 8, 9] and established experimentally [10, 11, 12]. The question is whether interference effects in 3D random dielectric media can reduce the diffusion constant to zero leading

[†]Presently on leave at Commissariat à l'Energie Atomique, DSM/DRECAM/SPAM, Centre d'Etudes de Saclay, 91191 Gif-sur-Yvette, France

to strong localization. The crucial parameter is the mean free path l which should be rather short [13, 14, 15].

Of course, apart from remarkable similarities between scattering of electrons and light waves, there are also striking differences. Very different is, e.g., the long-wavelength limit of elastic scattering. For electrons we have mainly s-wave scattering which is spatially isotropic and wavelength independent. For light we observe p-wave scattering. In this case there is forward-backward symmetry but scattering is non-isotropic. In inelastic scattering electrons change their energy but their total number is conserved. For light we have strong absorption and the intensity decreases. Moreover electrons are described by scalar wave functions (or two-component spinors if the spin is included). To describe correctly scattering and localization of electromagnetic waves we need to consider, in general, three-dimensional vector fields.

The Anderson localization of electromagnetic waves could be observed experimentally in the scaling properties of the transmission T. Imagine a slab of thickness L containing randomly distributed non-absorptive scatterers. Usually propagation of electromagnetic waves in weakly scattering random media can be described adequately by a diffusion process [16, 17]. Thus the equivalent of the Ohm's law holds and the transmission decreases linearly with the thickness of the sample, i.e., $T \propto L^{-1}$ (for sufficiently large L). However, when the fluctuations of the dielectric constant become large enough, the electromagnetic field ceases to diffuse and becomes localized due to interference. Anderson localization occurs when this happens. In such a case the material behaves as an optical equivalent of an insulator and the transmission decreases exponentially with the size of the system $T \propto e^{-L/\xi}$ [4, 18].

A convincing experimental demonstration that Anderson localization is indeed possible in three-dimensional disordered dielectric structures has been given recently [19]. The strongly scattering medium has been provided by semiconductor powders with a very large refractive index. By decreasing the average particle size it was possible to observe a clear transition from linear scaling of transmission ($T \propto L^{-1}$) to an exponential decay ($T \propto e^{-L/\xi}$). Some localization effects have been also reported in previous experiments on microwave localization in copper tubes filled with metallic and dielectric spheres [20]. However, the latter experiments were plagued by large absorption, which makes the interpretation of the data quite complicated.

Thus from the experimental point of view there are indeed some reasonable indications that strong localization could be possible in three-dimensional random dielectric structures. On the other hand, it would be desirable to have a reasonably simple yet realistic theoretical model providing deeper insight into localization of light. It concerns especially those problems where the polarization effects have to be taken into account. Such considerations should assume the vector character of electromagnetic fields from the very beginning. To achieve this goal in a consistent way they should be based directly on the Maxwell equations. On the other hand, they should be simple enough to provide calculations without too many too-crude approximations. In this chapter

we construct explicitly such a model for the three-dimensional localization of electromagnetic waves. The resulting model is thoroughly analyzed and its major consequences are elaborated.

The main advantage of the presented approach is that we do not need to perform any averaging over the disorder. Generally speaking, there is a temptation to apply averaging procedures as soon as "disorder" is introduced into the model. Averaging of the scattered intensity over some random variable leads to a transport theory of localization [21, 22, 23]. But "there is a very important and fundamental truth about random systems we must always keep in mind: no real atom is an average atom, nor is an experiment done on an ensemble of samples" [24]. What we really need to properly understand the existing experimental results are probability distributions, not averages. Indeed, to perform any mathematically meaningful averaging procedure the assumption of infinite medium is needed. On the other hand in all experiments we can study finite media only. Within our approach we can see how localization "sets in" for increasing number of scatterers by studying the probability densities of eigenvalues of some random matrices.

This chapter is organized as follows. In Sec. 1.2 we introduce the Lippmann-Schwinger integral equations as a very convenient and effective tool for studying scattering of light by bounded dielectric media. Using this formalism in Sec. 1.3 we present general considerations dealing with elastic scattering of light waves. They will be used in Sec. 1.5 to derive the explicit form of coupling between a point-like scatterer and the electric field of the wave incident on it. In Sec. 1.4 a definition of light waves localized in dielectric media is proposed and its consequences are elaborated. It is shown that a way of dealing with localized states in the formalism of Lippmann-Schwinger equations is to solve them as a homogeneous system of equations, i.e., for the incoming wave equal to zero. In Sec. 1.5 we recall the point-scatterer approximation and analyze the basic ideas behind it. A representation for the scatterer that fulfills the optical theorem rigorously and conserves energy in the scattering processes is derived. In Sec. 1.6 we arrive at the system of linear equations determining the polarization of the medium for a given incident wave. Eigenvalues of the random Green matrix corresponding to this set of equations are studied. The Breit-Wigner-type model of the single scatterer allows us to give a clear physical interpretation of the obtained results. In this particular case the real and imaginary parts of the eigenvalues of the Green matrix can be considered as first order approximations to the relative widths and positions of the resonances. In Sec. 1.7 a numerical scattering experiment is performed. The positions and widths of the resonances are compared with the values obtained in Sec. 1.6. In Sec. 1.8 self-averaging of the real parts of the eigenvalues emerging in the limit of an infinite medium is discovered numerically. This phenomenon is illustrated graphically and observed features are compared with one-dimensional results. Note that in one dimension the possibility of self-averaging can be proved analytically. In Sec. 1.9 a sound physical interpretation of the obtained results is proposed. Self-averaging of the real parts

of the eigenvalues is considered as the signature of the appearance of the band of localized electromagnetic waves, emerging in the limit of infinite system. It can be understood as a counterpart of Anderson localization in solid state physics. We finish with some comments and conclusions in Sec. 1.10.

1.2 BASIC ASSUMPTIONS

In the following we restrict ourselves to the study of the properties of the stationary solutions

$$\vec{E}(\vec{r},t) = \mathrm{Re}\left\{\vec{\mathcal{E}}(\vec{r})e^{-i\omega t}\right\}, \quad \vec{H}(\vec{r},t) = \mathrm{Re}\left\{\vec{\mathcal{H}}(\vec{r})e^{-i\omega t}\right\}, \tag{1.1}$$

of the Maxwell equations. Consequently, the polarization of the medium is considered to be the oscillatory function of time

$$\vec{P}(\vec{r},t) = \mathrm{Re}\left\{\vec{\mathcal{P}}(\vec{r})e^{-i\omega t}\right\}. \tag{1.2}$$

The polarization of the isotropic linear and lossless dielectric medium described by the real dielectric constant $\epsilon(\vec{r})$ is related to the electric field by the well-known relation [25]:

$$\vec{\mathcal{P}}(\vec{r}) = \frac{\epsilon(\vec{r})-1}{4\pi}\vec{\mathcal{E}}(\vec{r}). \tag{1.3}$$

Let us stress that in all experiments we can investigate only systems confined to certain finite regions of space. It is therefore reasonable to restrict our analysis to bounded media consisting of finite number of dielectric particles. In this case the polarization (1.3) satisfies the condition

$$\vec{\mathcal{P}}(\vec{r}) = 0 \quad \text{for} \quad |\vec{r}| > R. \tag{1.4}$$

Note, that in the above formula we have explicitly introduced the characteristic length-scale R which will be used later on. Denoting by $k = \omega/c$ the wavenumber in vacuum and introducing the complex Hertz vector

$$\vec{\mathcal{Z}}(\vec{r}) = \int d^3r' \vec{\mathcal{P}}(\vec{r'}) \frac{e^{ik|\vec{r}-\vec{r'}|}}{|\vec{r}-\vec{r'}|}, \tag{1.5}$$

the field scattered by the finite dielectric medium (1.4) can be written in the following form [26]:

$$\vec{\mathcal{E}}^{(1)}(\vec{r}) = \vec{\nabla}\times\vec{\nabla}\times\vec{\mathcal{Z}}(\vec{r}), \quad \vec{\mathcal{H}}^{(1)}(\vec{r}) = -ik\vec{\nabla}\times\vec{\mathcal{Z}}(\vec{r}). \tag{1.6}$$

The total field may now be considered as the sum of the scattered field (1.6) and the free field $\vec{\mathcal{E}}^{(0)}(\vec{r}), \vec{\mathcal{H}}^{(0)}(\vec{r})$:

$$\vec{\mathcal{E}}(\vec{r}) = \vec{\mathcal{E}}^{(0)}(\vec{r}) + \vec{\mathcal{E}}^{(1)}(\vec{r}), \quad \vec{\mathcal{H}}(\vec{r}) = \vec{\mathcal{H}}^{(0)}(\vec{r}) + \vec{\mathcal{H}}^{(1)}(\vec{r}). \tag{1.7}$$

The system of equations (1.3), (1.5), (1.6), and (1.7) fully determines the electromagnetic field $\vec{\mathcal{E}}(\vec{r}), \vec{\mathcal{H}}(\vec{r})$ everywhere in space for a given field of the free wave $\vec{\mathcal{E}}^{(0)}(\vec{r}), \vec{\mathcal{H}}^{(0)}(\vec{r})$ incident on the system. Analogous relationships between the stationary outgoing wave and the stationary incoming wave are known in the general scattering theory as the Lippmann-Schwinger equations [27].

Let us observe, that far from the medium, i.e., for $|\vec{r}| \gg R$ the Hertz vector (1.5) can be approximated by

$$\vec{\mathcal{Z}}(\vec{r}) \approx \vec{\mathcal{P}}(k\vec{n}) \frac{e^{ik|\vec{r}|}}{|\vec{r}|}, \tag{1.8}$$

where

$$\vec{\mathcal{P}}(\vec{k}) = \int d^3 r \vec{\mathcal{P}}(\vec{r}) e^{-i\vec{k}\cdot\vec{r}}, \tag{1.9}$$

is the spatial Fourier transform of the polarization and

$$\vec{n} = \frac{\vec{r}}{|\vec{r}|}, \tag{1.10}$$

is the versor pointing to the direction of observation. We see from Eq. (1.8) that for each direction of observation $\vec{n}$ the far-field scattered by the localized dielectric medium (1.4) looks like the field radiated by a certain Hertz dipole described by the polarization

$$\vec{\mathcal{P}}(\vec{r}) = \vec{\mathcal{P}}(k\vec{n}) \delta(\vec{r}). \tag{1.11}$$

1.3 ELASTIC SCATTERING

We are interested in lossless media only, where localization is due to interference effects in elastic scattering of light by various parts of the medium. It is obvious, that if the bounded dielectric medium (1.4) is lossless, then the time-averaged field energy flux integrated over a surface surrounding it should vanish:

$$\int d\vec{s} \cdot \vec{\mathcal{S}}(\vec{r}) = \frac{c}{4\pi} \frac{1}{2} \mathrm{Re} \int d\vec{s} \cdot \left\{ \vec{\mathcal{E}}(\vec{r}) \times \vec{\mathcal{H}}^*(\vec{r}) \right\} = 0. \tag{1.12}$$

It turns out, that the energy conservation condition (1.12) leads to restrictions imposed on the polarization $\vec{\mathcal{P}}(\vec{r})$. As we will see in the present section, the requirement that the time-averaged total-field energy flux integrated over

a surface surrounding the considered bounded and lossless medium should vanish for the arbitrary incident wave $\vec{\mathcal{E}}^{(0)}(\vec{r})$, $\vec{\mathcal{H}}^{(0)}(\vec{r})$ determines uniquely the form of the dependence of the polarization of the medium on the field. The results of those general considerations dealing with elastic scattering by bounded dielectric media will be used in Sec. 1.5 to derive of the explicit form of the coupling between the point-like scatterer and the electric field of the light wave incident on it.

After inserting the formula (1.7), the expression (1.12) may be splited into three terms. The first term

$$\int d\vec{s}\cdot\vec{\mathcal{S}}^{(1)}(\vec{r}) = \frac{c}{4\pi}\frac{1}{2}\mathrm{Re}\int d\vec{s}\cdot\left\{\vec{\mathcal{E}}^{(1)}(\vec{r})\times\vec{\mathcal{H}}^{(1)*}(\vec{r})\right\}, \tag{1.13}$$

corresponds to the time-averaged energy radiated by the medium per unit time. To obtain its explicit form we use the formula for the Poynting vector of the field radiated by the Hertz dipole (1.11) in the far-field limit (see, e.g., [26]):

$$\vec{\mathcal{S}}^{(1)}(\vec{r}) = \vec{n}\frac{1}{8\pi}\frac{ck^4}{|\vec{r}|^2}|\vec{\mathcal{P}}_T(k\vec{n})|^2, \tag{1.14}$$

where

$$\vec{\mathcal{P}}_T(\vec{k}) = \vec{\mathcal{P}}(\vec{k}) - \frac{\vec{k}(\vec{k}\cdot\vec{\mathcal{P}}(\vec{k}))}{|\vec{k}|^2}, \tag{1.15}$$

denotes the transverse part of the Fourier transform of the polarization. Integrating Eq. (1.14) over a sphere with radius $|\vec{r}|$ surrounding all sources we get the following expression for the energy radiated at average by the dielectric medium (1.4):

$$\int d\vec{s}\cdot\vec{\mathcal{S}}^{(1)}(\vec{r}) = \frac{ck^4}{8\pi}\int d\Omega|\vec{\mathcal{P}}_T(k\vec{n})|^2. \tag{1.16}$$

The second term describes the total time-averaged energy flux integrated over a closed surface for the free field and thus vanishes

$$\frac{c}{4\pi}\frac{1}{2}\mathrm{Re}\int d\vec{s}\cdot\left\{\vec{\mathcal{E}}^{(0)}(\vec{r})\times\vec{\mathcal{H}}^{(0)*}(\vec{r})\right\} = 0. \tag{1.17}$$

To calculate the last interference term

$$\frac{c}{4\pi}\frac{1}{2}\mathrm{Re}\int d\vec{s}\cdot\left\{\vec{\mathcal{E}}_0(\vec{r})\times\vec{\mathcal{H}}^{(1)*}(\vec{r}) + \vec{\mathcal{E}}^{(1)}(\vec{r})\times\vec{\mathcal{H}}^{(0)*}(\vec{r})\right\}, \tag{1.18}$$

we use the following identity (Lorentz theorem)

$$\vec{\nabla}\cdot\left\{\vec{\mathcal{E}}^{(0)}(\vec{r})\times\vec{\mathcal{H}}^{(1)*}(\vec{r}) + \vec{\mathcal{E}}^{(1)*}(\vec{r})\times\vec{\mathcal{H}}^{(0)}(\vec{r})\right\} = -4\pi ik\vec{\mathcal{P}}^*(\vec{r})\cdot\vec{\mathcal{E}}^{(0)}(\vec{r}), \tag{1.19}$$

which follows directly from the Maxwell equations. Integrating (1.19) over a volume containing the isolated part of the medium under consideration and

calculating the real part we see that the Eq. (1.12) may be written in an equivalent form

$$\int d\vec{s}\cdot\vec{\mathcal{S}}^{(1)}(\vec{r}) = \frac{1}{2}ck\mathrm{Re}\int d^3r\left\{i\vec{\mathcal{P}}^*(\vec{r})\cdot\vec{\mathcal{E}}^{(0)}(\vec{r})\right\}. \tag{1.20}$$

Thus on average the energy radiated by the medium must be equal to the energy given to the medium by the incident wave. The condition (1.20) together with Eq. (1.16) determines the relation between polarization and the electric field of the incident wave. It may be viewed as a generalized version of the optical theorem.

1.4 LOCALIZED WAVES

The standard approach to localized electromagnetic waves [3, 15, 28, 29, 30, 31, 32, 33] is based on the similarities between the Helmholtz equation for the electric field amplitude in an isotropic lossless dielectric

$$\vec{\nabla}\times\vec{\nabla}\times\vec{\mathcal{E}}(\vec{r}) + k^2[1-\epsilon(\vec{r})]\vec{\mathcal{E}}(\vec{r}) = k^2\vec{\mathcal{E}}(\vec{r}), \tag{1.21}$$

and the time-independent Schrödinger equation

$$\left\{-\frac{\hbar^2}{2m}\nabla^2 + V(\vec{r})\right\}\psi(\vec{r}) = E\psi(\vec{r}). \tag{1.22}$$

The term $k^2[1-\epsilon(\vec{r})]$ corresponds to the potential $V(\vec{r})$ providing localization of the electron wave function and the squared wave number in vacuum $k^2 = \omega^2/c^2$ plays the role analogous to the energy eigenvalue E. By definition, an electromagnetic wave is localized in a certain region of space if its magnitude is (at least) exponentially decaying in any direction from this region. We will show now that electromagnetic waves localized in the finite dielectric medium (1.4) correspond to nonzero solutions $\vec{\mathcal{E}}(\vec{r}) \neq 0$ of Eqs. (1.3), (1.5), (1.6), and (1.7) for the incoming wave equal to zero, i.e., $\vec{\mathcal{E}}^{(0)}(\vec{r}) \equiv 0$.

Indeed, let us suppose that the field is exponentially localized in the vicinity of the bounded dielectric medium (1.4). First let us observe that, due to Eqs. (1.6) and (1.8), the scattered field $\vec{\mathcal{E}}^{(1)}(\vec{r})$, $\vec{\mathcal{H}}^{(1)}(\vec{r})$ tends to zero if $|\vec{r}| \to \infty$. Thus if the total field (1.7) is exponentially localized, then the free field $\vec{\mathcal{E}}^{(0)}(\vec{r}), \vec{\mathcal{H}}^{(0)}(\vec{r})$ must also tend to zero in this limit. But it is known from the vector form of the Kirchhoff integral formula [25] that if the free field vanishes on a closed surface, then it is zero everywhere inside this surface.

The proof works also the other way round. Suppose that $\vec{\mathcal{E}}(\vec{r})$ is a solution of Eqs. (1.3), (1.5), (1.6), and (1.7) for $\vec{\mathcal{E}}^{(0)}(\vec{r}) \equiv 0$. For $z > R$ (the choice of the z axis is arbitrary) the scattered field $\vec{\mathcal{E}}^{(1)}(\vec{r})$ can be expanded into the plane waves propagating into the positive z direction and the evanescent

plane waves:

$$\vec{\mathcal{E}}^{(1)}(\vec{r}) = \int \frac{d^2q}{(2\pi)^2} \vec{A}(\vec{q}) e^{i\vec{k}\cdot\vec{r}}, \quad \text{where} \quad \vec{k} = \left[q_x, q_y, \sqrt{k^2 - |\vec{q}|^2}\right]. \tag{1.23}$$

Using the Lorentz theorem Eq. (1.19) and performing the straightforward but lengthly calculations (see, e.g., [25]) we easily arrive at the following expressions determining the coefficients $\vec{A}(\vec{q})$ corresponding to the propagating waves:

$$\vec{A}(\vec{q}) = 2\pi i k \vec{\mathcal{P}}_T(\vec{k}), \quad \text{where} \quad |\vec{q}| < k. \tag{1.24}$$

As the considered medium is non-dissipative, the time average energy stream integrated over a closed surface surrounding it must vanish:

$$\int d\vec{s} \cdot \vec{\mathcal{S}}^{(1)}(\vec{r}) = 0. \tag{1.25}$$

Inserting (1.16) into the condition (1.25) we see that the transverse part of the polarization of the medium vanishes on the light cone

$$\vec{\mathcal{P}}_T(\vec{k}) = 0, \quad \text{for} \quad |\vec{k}| = k. \tag{1.26}$$

This means that there are no propagating plane waves in the scattered field (which in the case $\vec{\mathcal{E}}^{(0)}(\vec{r}) \equiv 0$ is equal to the total field). Therefore the field consists only of evanescent plane waves and thus is exponentially localized.

1.5 POINT-SCATTERERS

Usually localization of light is studied experimentally in microstructures consisting of dielectric spheres with diameters and mutual distances being comparable to the wavelength [15]. It is well known, that the theory of multiple scattering of light by dielectric particles is tremendously simplified in the limit of point scatterers. In principle, this approximation is justified only when the size of the scattering particles is much smaller than the wavelength. In practical calculations, however, many multiple-scattering effects can be obtained qualitatively for coupled electrical dipoles. Examples are: universal conductance fluctuations [34], enhanced backscattering [35], dependent scattering [36], and strong localization in two [37, 38] and three dimensions [39, 40]. We believe that what really counts for localization is the scattering cross-section and not the geometrical shape and real size of the scatterer. Therefore we will represent the dielectric particles located at the points $\vec{r}_a$ by *single* electric dipoles

$$\vec{\mathcal{P}}(\vec{r}) = \sum_a \vec{p}_a \delta(\vec{r} - \vec{r}_a), \tag{1.27}$$

with properly adjusted scattering properties.

Let us mention that in practice any dielectric medium may be modeled by a set of discrete electric dipoles. This so-called coupled-dipole approximation was successfully used to study light scattering by a dielectric sphere [41] and more recently to obtain the scattering coefficients of arbitrarily shaped particles [42]. This method works well only if there are many dipoles in a volume whose dimensions are of the order of the wavelength [26]. In numerical calculations performed on supercomputers, a single small dielectric particle is built out of about a 10^6 dipoles (see, e.g. [43]). This is an important difference between the coupled-dipole approximation and our qualitative approach. In our case a single dielectric particle with diameter comparable to the wavelength is modeled only by *one* dipole with properly adjusted scattering properties.

It is known that several mathematical problems emerge in the formulation of interactions of point-like dielectric particles with electromagnetic waves [36, 44, 45]. Instead of applying several complicated regularization procedures we will shown that it is possible to analyze light scattering by point-like dielectric particles as a special case of general considerations dealing with elastic scattering of electromagnetic waves presented in Sec. 1.3. Previous results corresponding to the two-dimensional case were based on the Kirchhoff integral formula for scalar waves. We are interested in lossless media only, where localization is due to interference effects in elastic scattering of light by various dielectric particles. Therefore the time-averaged Poynting vector integrated over a surface surrounding each scatterer must vanish for the arbitrary incident wave. As was shown in Sec. 1.3, this condition will be fulfilled if the dipole moments $\vec{p}_a$ depend on the electric field of the wave incident on them.

To obtain an explicit form of the coupling let us recall the formula for the energy radiated on average by the Hertz dipole [26]:

$$\int d\vec{s}\cdot\vec{\mathcal{S}}^{(1)}(\vec{r}) = \frac{1}{3}ck^4|\vec{p}|^2, \tag{1.28}$$

which can be derived by substituting the polarization of a point-scatterer into Eq. (1.16) and performing the straightforward integration. Inserting the above expression and the Eq. (1.27) we may rewrite the condition (1.20) in the following form

$$\left|ik^3\vec{p}_a + \frac{3}{4}\vec{\mathcal{E}}'(\vec{r}_a)\right|^2 = \left|\frac{3}{4}\vec{\mathcal{E}}'(\vec{r}_a)\right|^2, \tag{1.29}$$

where the field acting on the ath scatterer

$$\vec{\mathcal{E}}'(\vec{r}_a) = \vec{\mathcal{E}}^{(0)}(\vec{r}_a) + \sum_{b\neq a}\vec{\mathcal{E}}_b(\vec{r}_a), \tag{1.30}$$

is the sum of the free field and waves scattered by all other particles

$$\vec{\mathcal{E}}_a(\vec{r}) = \frac{2}{3} i k^3 \hat{g}(\vec{r} - \vec{r}_a) \cdot \vec{p}_a, \tag{1.31}$$

which are expressed by the Green tensor (see, e.g., [26]):

$$\hat{g}(\vec{r}) = \frac{3}{2} \frac{e^{ik|\vec{r}|}}{ik|\vec{r}|} \left\{ \left(\frac{3}{(k|\vec{r}|)^2} - i\frac{3}{k|\vec{r}|} - 1 \right) \frac{\vec{r}\vec{r}}{|\vec{r}|^2} - \left(\frac{1}{(k|\vec{r}|)^2} - i\frac{1}{k|\vec{r}|} - 1 \right) \right\}. \tag{1.32}$$

Assuming that the vector on the left hand side of Eq. (1.29) is a function of the vector on the right hand side and that the dielectric particles modeled by the dipoles are spherically symmetrical we get

$$\frac{2}{3} i k^3 \vec{p}_a = \frac{1}{2}(e^{2i\phi} - 1)\vec{\mathcal{E}}'(\vec{r}_a). \tag{1.33}$$

Thus, to provide conservation of energy, the dipole moments are coupled to the electric field of the incident wave by complex "polarizability" $(e^{2i\phi} - 1)/2$, which can take values from a circle on the complex plane.

Dividing Eq. (1.28) by the intensity of a plane wave given by [26]:

$$I = \frac{c}{8\pi} |\vec{\mathcal{E}}^{(0)}(\vec{r}_a)|^2 \tag{1.34}$$

and inserting Eq. (1.33) we obtain the explicit formula for the total scattering cross-section σ of an individual scatterer:

$$k^2\sigma = 6\pi \sin^2 \phi. \tag{1.35}$$

The scatterers necessarily have an internal structure. Thus in general the phase shift ϕ from Eq. (1.33) should be regarded as a function of frequency ω. For example to model a simple scatterer with one internal Breit-Wigner type resonance one can write:

$$\cot \phi = -\frac{\omega - \omega_0}{\gamma_0}. \tag{1.36}$$

The total scattering cross-section σ takes then the familiar Lorentzian form:

$$k^2\sigma = \frac{6\pi\gamma_0^2}{(\omega - \omega_0)^2 + \gamma_0^2}. \tag{1.37}$$

1.6 EIGENPROBLEM

Now, inserting Eq. (1.31) into (1.30), and using (1.33), it is easy to obtain the system of linear equations determining the field acting on each dipole $\vec{\mathcal{E}}'(\vec{r}_a)$

for a given incoming wave $\vec{\mathcal{E}}^{(0)}(\vec{r}_a)$:

$$\vec{\mathcal{E}}'(\vec{r}_a) = \vec{\mathcal{E}}^{(0)}(\vec{r}_a) + \frac{e^{2i\phi}-1}{2}\sum_b \hat{G}_{ab}\cdot\vec{\mathcal{E}}'(\vec{r}_b). \tag{1.38}$$

The elements of the $\hat{G}$ matrix from Eq. (1.38) are equal to the Green function calculated for the differences between the positions of the scatterers:

$$\hat{G}_{ab} = \begin{cases} \hat{g}(\vec{r}_a - \vec{r}_b) & \text{for } a \neq b \\ 0 & \text{for } a = b \end{cases}. \tag{1.39}$$

If we solve Eqs. (1.38) and use again Eq. (1.33) to find $\vec{p}_a$, then we are able to find the electromagnetic field everywhere in space.

A way of dealing with *resonances* in this formalism is to look for resonance poles in the complex ω plane. Resonance poles are frequencies ω for which it is possible to solve Eqs. (1.38) as a homogeneous equations, i.e., for the incoming wave $\vec{\mathcal{E}}^{(0)}$ equal to zero. The real and imaginary parts of the resonance frequencies determine the positions and widths of the resonances. This method has been applied recently to the analysis of resonances in a system of $N = 2$ s-wave scatterers [46, 47]. An example of such a system is the case of fixed frequency sound incident on small identical air bubbles in water [48, 49, 50]. Electron or phonon scattering from defects or impurities in crystal lattices give another example. It turned out that very interesting phenomena can arise for pair of identical scatterers placed very close together, well within one wavelength. An extremely narrow p-wave *proximity* resonance develops from a broad s-wave resonance of individual scatterers. A new s-wave resonance of the pair also appears [46]. A similar problem of scattering of light from two spherical particles has been discussed by Vadim Markel [51].

It is seen from Eqs. (1.38) that for $\vec{\mathcal{E}}^{(0)} \equiv 0$ the latter system of equations is equivalent to the *eigenproblem* for the $\hat{G}$ matrix:

$$\sum_{b=1}^{N} \hat{G}_{ab}\cdot\vec{\mathcal{E}}'(\vec{r}_b) = \lambda\vec{\mathcal{E}}'(\vec{r}_a), \quad a = 1,\ldots,N \tag{1.40}$$

where

$$\lambda = -1 - i\cot\phi. \tag{1.41}$$

The Green matrix defined by Eq. (1.39) depends only on the the scaled distances between all pairs of the scatterers $k|\vec{r}_a - \vec{r}_b|$. Therefore for fixed positions of the scatters $\vec{r}_a$, its eigenvalues still remain functions of frequency ω. Using an explicit model of the scattering phase shift $\phi(\omega)$ and solving Eq. (1.41) in a complex ω plane it is possible to determine the positions and widths of the resonances. In the particular case of the Breit-Wigner type scatterers Eq. (1.36) the real and imaginary parts of the eigenvalues of the $\hat{G}$ matrix have a nice physical interpretation: they are equal to the relative

widths $(\gamma-\gamma_0)/\gamma_0$ and positions $(\omega-\omega_0)/\gamma_0$ of the resonances. Indeed, using the explicit form of the complex frequency $\omega \to \omega - i\gamma$ and substituting the Breit-Wigner model of the scattering into Eq. (1.41) we get:

$$\omega - i\gamma = \omega_0 - i\gamma_0[1 + \lambda(\omega - i\gamma)] \tag{1.42}$$

This system of two coupled nonlinear equations determines the values of the resonance poles $\omega - i\gamma$. In many physically interesting cases Eqs. (1.42) can be solved numerically by iteration. For instance in solving it up to the first order in γ_0/ω_0 one substitutes $\lambda(\omega_0)$ for $\lambda(\omega - i\gamma)$ getting:

$$\mathrm{Re}\lambda(\omega_0) \simeq \frac{\gamma-\gamma_0}{\gamma_0}, \quad \mathrm{Im}\lambda(\omega_0) \simeq \frac{\omega-\omega_0}{\gamma_0}. \tag{1.43}$$

Let us start with a simplest possible example of a system of $N = 2$ scatterers separated by a distance d. In this case the $\hat{G}$ matrix from Eq. (1.39) has four eigenvalues: $\lambda_{\pm}^{(T)} = \mp\frac{3}{2}\frac{e^{ikd}}{ikd}\left(\frac{1}{(kd)^2} - i\frac{1}{kd} - 1\right)$ corresponding to the transverse oscillations of the dipoles, and $\lambda_{\pm}^{(L)} = \pm\frac{3}{2}\frac{e^{ikd}}{ikd}\left(\frac{2}{(kd)^2} - i\frac{2}{kd}\right)$ corresponding to the longditual oscillations of the dipoles. The upper sign $(+)$ describes oscillations in phase, whereas the lower sign $(-)$ corresponds to the oscillations in anti-phase. For $k = k_0 = \omega_0/c$ the eigenvalues $\lambda_{\pm}^{(T)}$ and $\lambda_{\pm}^{(L)}$ may be considered as an approximate solution of Eq. (1.42) up to the first order in γ_0/ω_0.

The eigenvalues $\lambda_{\pm}^{(T)}$ and $\lambda_{\pm}^{(L)}$ are depicted in Fig. 1.1. They form a characteristic four-arms spiral. We see that for scatterers very close to each other $(d \to 0)$ two arms of this spiral corresponding to the oscillations in anti-phase approach the axis $\mathrm{Re}\lambda = -1$ $(\gamma = 0)$. They are related to the very narrow "antisymmetric" resonances. On the other hand in this limit the remaining two arms corresponding to the oscillations in phase tend asymptotically to the axis $\mathrm{Re}\lambda = 1$ $(\gamma = 2\gamma_0)$. These arms are related to the "symmetric" resonances of the pair which are about twice as broad as the resonance of the single scatterer. For $d \to \infty$ both arms meet in the point $\lambda = 0$ $(\omega = \omega_0, \gamma = \gamma_0)$ reproducing the results of the single scattering.

As a second example let us consider systems of $N = 100$ and $N = 1000$ scatterers placed randomly inside a sphere, with the uniform density $n = 1$ scatterer per wavelength cubed l_0^3. The chosen wavelength, l_0, corresponds to the resonance frequency ω_0 (i.e., $l_0 = 2\pi/k_0$ where $k_0 = \omega_0/c$). In Figs. 1.2 and 1.3 we plot the eigenvalues λ obtained after numerically diagonalizing the corresponding $\hat{G}$ matrices. In the case of the Breit-Wigner type scatterers these eigenvalues can be considered as the approximate positions of the resonance poles up to the first order in γ_0/ω_0. Comparing Figs. 1.2 and 1.3 with Fig. 1.1 we see that the tails corresponding to "antisymmetric" proximity resonances still persists for a larger number of scatterers. On the other hand the remaining two arms of the spiral from Fig. 1.1 corresponding to the

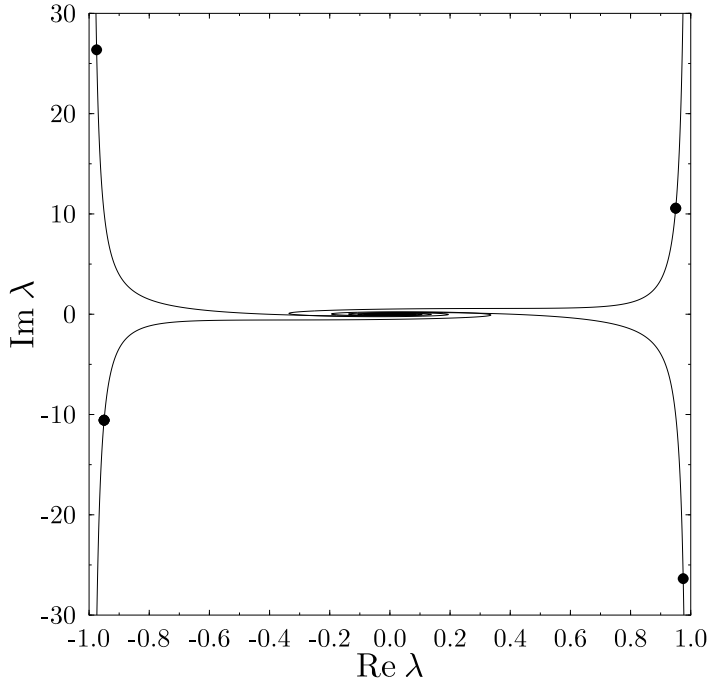

Fig. 1.1 Eigenvalues λ of a $\hat{G}$ matrix corresponding to a system of $N = 2$ point-like scatterers. All four types of resonances all clearly visible. The four black dots correspond to the eigenvalues calculated for a certain specific value of the distance between the scatterers kd.

"symmetric" resonances between pairs of scatterers completely disappeared in the case of $N = 1000$. It follows also from inspection of Figs. 1.2 and 1.3 that for increasing number of scatterers new collective effects start to appear. They are visible especially for $\mathrm{Im}\lambda \simeq 0$, i.e., for frequencies which are close to the resonance frequency of a single scatterer ($\omega \simeq \omega_0$). For instance in this range of frequencies quite a lot of eigenvalues are located near the $\mathrm{Re}\lambda = -1$ ($\gamma = 0$) axis. They correspond to narrow resonances with width $\gamma \simeq .25\gamma_0$. As we will show in a moment, width of these resonances γ decreases with increasing number of scatterers N (while keeping the density constant) and in the limit of the infinite medium $N \to \infty$ they become localized states. It is also seen from Fig. 1.3 that a few new broad (i.e., $\gamma \simeq 2.5\gamma_0$) resonances appear for $\omega \simeq \omega_0$ in this limit.

Looking for resonance poles in a complex energy plane turns out to be an enormous numerical problem for a large number of scatterers. Nevertheless, as we have seen in the case of $N = 2$ Breit-Wigner type scatterers, sometimes it is possible to extract some qualitative information about the resonances just from the spectrum of the $\hat{G}$ matrix calculated for real values of energy. Moreover, as will be shown in Sec. 1.8, a striking phase-transition-like behavior appears in the spectra of such a Green matrices when the number of scatterers increases. This transition may be interpreted as an appearance of the band of localized states emerging in the limit of the infinite medium. It is an interesting analog of the Anderson localization in noncrystalline solids such as amorphous semiconductors or disordered metals.

1.7 SCATTERING EXPERIMENT

The actual properties of physical systems have to be observed experimentally and it is not enough just to know the properties of the stationary solutions of the Maxwell equations. These are only theoretical tools. Experiments deal rather with measurable quantities and, for many practical problems, a natural quantity to look for is the total scattering cross-section of a finite system σ and its dependence on the frequency ω. In this section we would like to compare the positions and widths of the resonances of the total scattering cross-section of a system of point-like scatterers with the approximate positions of the complex resonance poles calculated in Sec. 1.6.

Inserting into Eq. (1.20) the free field in the form of a plane wave:

$$\vec{\mathcal{E}}^{(0)}(\vec{r}) = \vec{\mathcal{E}}^{(0)}(0)e^{i\vec{k}\cdot\vec{r}}, \tag{1.44}$$

substituting Eq. (1.27), using Eq. (1.33), dividing the resulting equation by the intensity of the incident wave Eq. (1.34), and assuming $|\vec{\mathcal{E}}^{(0)}(0)|^2 = 1$ we arrive at the explicit formula for the total scattering cross-section σ of a

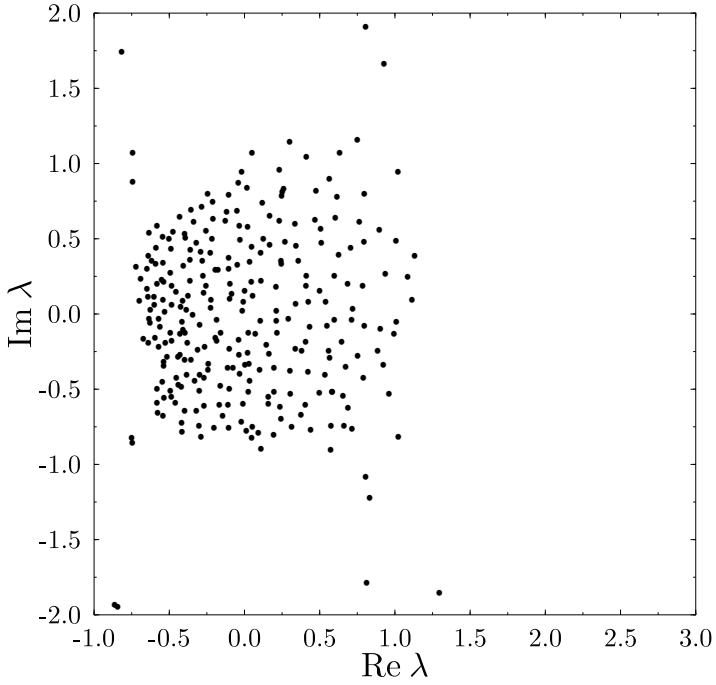

Fig. 1.2 Eigenvalues λ of a $\hat{G}$ matrix corresponding to a certain specific configuration of $N = 100$ point-like scatterers placed randomly inside a sphere, with uniform density $n = 1$ scatterer per wavelength cubed. The tails corresponding to "symmetric" and "antisymmetric" proximity resonances from Fig. 1.1 still persist.

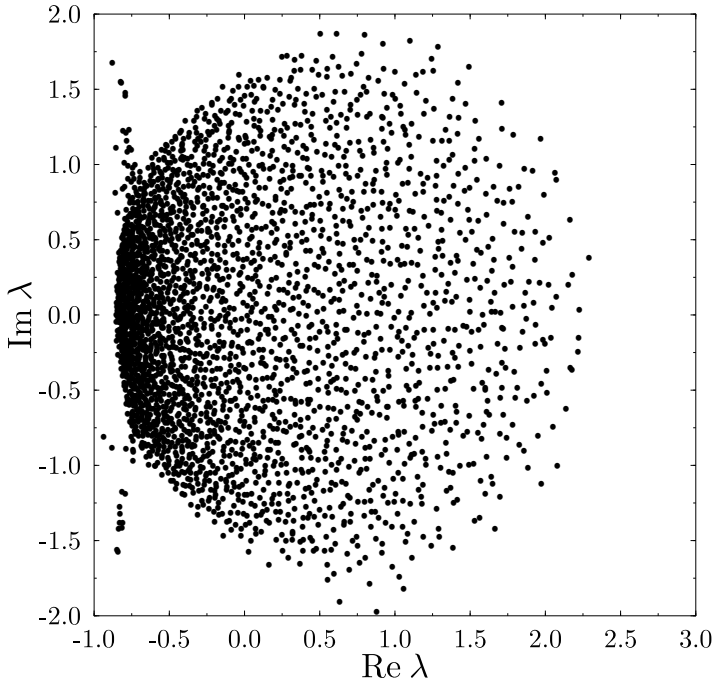

Fig. 1.3 Eigenvalues λ of a $\hat{G}$ matrix corresponding to a certain specific configuration of $N = 1000$ point-like scatterers placed randomly inside a sphere, with uniform density $n = 1$ scatterer per wavelength cubed. Quite a lot of eigenvalues are located near the $\mathrm{Re}\lambda = -1$ axis.

system of N identical point-like scatterers:

$$k^2\sigma = -6\pi \mathrm{Re}\left\{\frac{e^{2i\phi}-1}{2}\sum_{a=1}^{N}\vec{\mathcal{E}}'(\vec{r}_a)\cdot\vec{\mathcal{E}}'^{(0)*}(\vec{r}_a)\right\}. \tag{1.45}$$

By substituting $\vec{\mathcal{E}}'^{(0)}(\vec{r}_a)$ from Eq. (1.30) after lengthly but straightforward calculations it is possible to rewrite Eq. (1.45) in an equivalent way:

$$k^2\sigma = 6\pi \sin^2\phi \sum_{a=1}^{N}\sum_{b=1}^{N}\vec{\mathcal{E}}'(\vec{r}_a)\cdot \mathrm{Re}\left\{\hat{g}(\vec{r}_a-\vec{r}_b)\right\}\cdot\vec{\mathcal{E}}'^{*}(\vec{r}_b). \tag{1.46}$$

Eq. (1.46) can also be derived by substituting the polarization of a system of point-scatterers (1.27) into Eq. (1.16), using Eq. (1.33) and explicitly performing the integration over the solid angle.

Let us now suppose that $\vec{\mathcal{E}}'(\vec{r}_a)$ is an eigenvector of the $\hat{G}$ matrix corresponding to the eigenvalue λ. In this case Eq. (1.30) reduces to:

$$\left\{1-\frac{e^{2i\phi}-1}{2}\lambda\right\}\vec{\mathcal{E}}'(\vec{r}_a) = \vec{\mathcal{E}}'^{(0)}(\vec{r}_a), \quad a=1,\ldots,N \tag{1.47}$$

and Eq. (1.46) takes the following form:

$$\begin{aligned} k^2\sigma &= \frac{6\pi}{(\cot\phi+\mathrm{Im}\lambda)^2+(1+\mathrm{Re}\lambda)^2}\times \\ &\sum_{a=1}^{N}\sum_{b=1}^{N}\vec{\mathcal{E}}^{(0)}(\vec{r}_a)\cdot \mathrm{Re}\left\{\hat{g}(\vec{r}_a-\vec{r}_b)\right\}\cdot\vec{\mathcal{E}}^{(0)*}(\vec{r}_b). \end{aligned} \tag{1.48}$$

Therefore the scattering cross-section σ considered as a function of $\cot\phi$ for a constant value of the frequency ω has a form of a Lorentzian curve of width $\mathrm{Re}\lambda+1$ centered at $\mathrm{Im}\lambda = -\cot\phi$. Note, that for Breit-Wigner type scatterers Eq. (1.36) we have $(\omega-\omega_0)/\gamma_0 = -\cot\phi$. Thus, in this particular case, the plot of σ as a function of $-\cot\phi$ computed for $\omega=\omega_0$ may be considered as an approximation to the plot of σ as a function of $(\omega-\omega_0)/\gamma_0$ up to the first order in γ_0/ω_0. Therefore Eq. (1.48) is consistent with results of Sec. 1.6, where we have shown that in the case of Breit-Wigner type scatterers the first order approximations to the relative widths $(\gamma-\gamma_0)/\gamma_0$ and positions $(\omega-\omega_0)/\gamma_0$ of the resonances are given by the real and imaginary parts of the eigenvalues of the $\hat{G}$ matrix calculated for $\omega=\omega_0$.

In Fig. 1.4 we have the scattering cross-section σ of a system of $N=2$ point-like scatterers ploted as a function of $-\cot\phi$. The system was illuminated by a linearly polarized plane wave. This plot corresponds to the certain specific configuration of scatterers from Fig. 1.1. The dashed line shows the scattering cross-section of an individual scatterer given by Eq. (1.35). We see from inspection of Fig. 1.4 that all four types of resonances are clearly visible. From

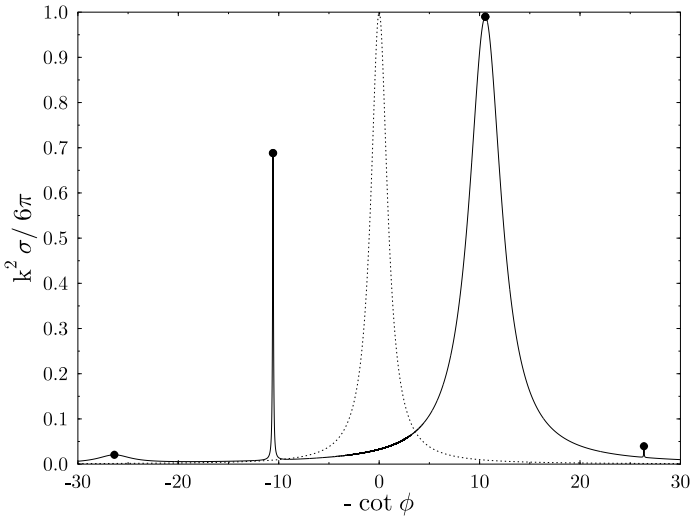

Fig. 1.4 Scattering cross-section σ of a certain specific configuration of $N = 2$ point-like scatterers from Fig. 1.1 ploted as a function of $-\cot\phi$. The dashed line corresponds to the scattering cross-section of an individual scatterer. All four types of resonances are clearly visible.

the left to right we have maxima of the scattering cross-section corresponding to the resonances related to the longditual oscillations in phase, transverse oscillations in anti-phase, transverse oscillations in phase, and longditual oscillations in anti-phase. The difference in strength between the transverse and longditual oscillations follows from the orientation of the system with respect to the polarization of the incident wave. The black dots in Fig. 1.4 mark the positions of the resonances calculated from the eigenvalues depicted as black dots in Fig. 1.1 by using the formula $\mathrm{Im}\lambda = -\cot\phi$.

In Fig. 1.5 we present the scattering cross-section σ/N of systems of $N = 100$ and 1000 point-like scatterers from Figs. 1.2 and 1.3 ploted as a function of $-\cot\phi$. For comparison we include also a plot of the scattering cross-section of an individual scatterer. The narrow collective resonances from Figs. 1.2 and 1.3 are not visible. A possible reason for this is that the corresponding eigenvectors of the $\hat{G}$ matrix are orthogonal to the vector formed by the values of incident field calculated at the positions of the scatterers. Nevertheless the appearance of a very broad collective resonance is readily seen. Note that in the case of a system of N scatterers scattering incoherently the total scattering cross-section of the system should scale as N, i.e, $\sigma/N = \text{const}$. It is seen

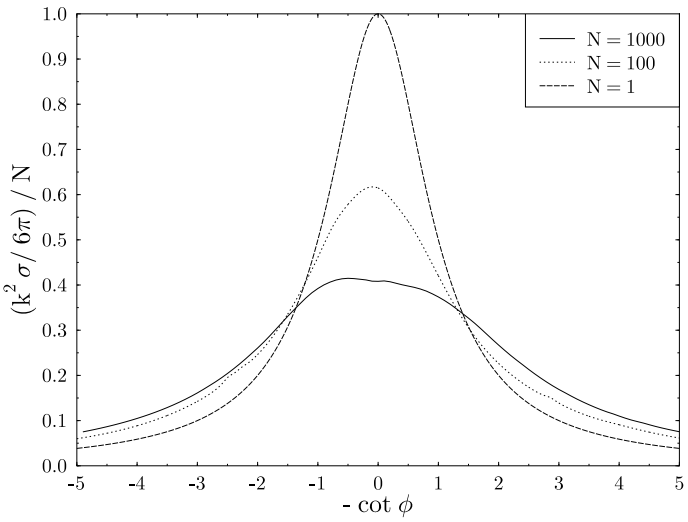

Fig. 1.5 Scattering cross-section σ of systems of $N = 100$ and 1000 point-like scatterers from Figs. 1.2 and 1.3 ploted as a function of $-\cot\phi$. The dashed line corresponds to the scattering cross-section of an individual scatterer. A very broad collective resonance appears for an increasing number of scatters. It can be considered as a precursor of the Anderson localization.

from Fig. 1.5 that for $|\cot\phi| < 1$ (or $|\omega - \omega_0| < \gamma_0$ in the case of Breit-Wigner scatterers) the scattering cross-section of a system is below this incoherent limit. On the other hand for $|\cot\phi| > 1$ (or $|\omega - \omega_0| > \gamma_0$ in the case of Breit-Wigner scatterers) we observe enhanced coherent scattering. It may be considered as a precursor of the Anderson localization.

1.8 SELF-AVERAGING

To illustrate the appearance of the band of localized electromagnetic waves, emerging in the limit of infinite system, we have to study the properties of *finite* systems for increasing number of dipoles N (while keeping the density constant). For each distribution of the dipoles $\vec{r}_a$ placed randomly inside a sphere with the uniform scaled density $n = 1$ dipole per wavelength cubed we have diagonalized numerically the $\hat{G}$ matrix from Eq. (1.39) and obtained the complex eigenvalues λ. The resulting probability distribution $P(\lambda)$, calculated from several different distributions of N dipoles is normalized in the standard way $\int d^2\lambda P(\lambda) = 1$. Let us now compare the surface plots of $P(\lambda)$ (treated as a function of two variables $\mathrm{Re}\lambda$ and $\mathrm{Im}\lambda$) calculated for systems consisting of $N = 100$ and 1000 dipoles. They are presented in Figs. 1.6 and 1.7, respectively. It is seen from inspection of these plots that, for increasing size of the system (in our case it increased $\sqrt[3]{10} \simeq 2$ times), at some $\mathrm{Im}\lambda$ the probability distribution $P(\lambda)$ apparently moves towards the $\mathrm{Re}\lambda = -1$ axis and simultaneously its variance decreases. This tendency is easily seen, e.g., for values of $|\mathrm{Im}\lambda|$ that are close to 0. Our numerical investigations indicate, that in the limit of an infinite medium, the probability distribution $P(\lambda)$ tends to the delta function in $\mathrm{Re}\lambda$:

$$\lim_{N\to\infty} P(\lambda) = \delta(\mathrm{Re}\lambda + 1) f(\mathrm{Im}\lambda). \tag{1.49}$$

We have some numerical evidence that this fact is a general property of $\hat{G}$ matrices, not restricted to the considered case of one dipole per wavelength cubed $n = 1$. Of course we could justify Eq. (1.49) by more orthodox approach based on a version of the finite size scaling analysis which leads however to an analogous conclusion.

It follows from Eq. (1.49) that in the limit $N \to \infty$ the distribution function $P(\lambda)$ has only one value of $\mathrm{Re}\lambda$ for which it is non-zero. The quantity $\mathrm{Re}\lambda$ is then "self-averaging" and the random process has in fact become deterministic. Knowledge of the average then provides knowledge about "almost every" individual realization of the random system. This property implies that the average value applies to *every single* realization of the system except for a few special ones (with measure zero). This means that for almost any random distribution of the dipoles $\vec{r}_a$, the equation $\mathrm{Re}\lambda = -1$ holds. Therefore Eq. (1.41) can be fulfilled if the phase shift of the scatterers satisfies:

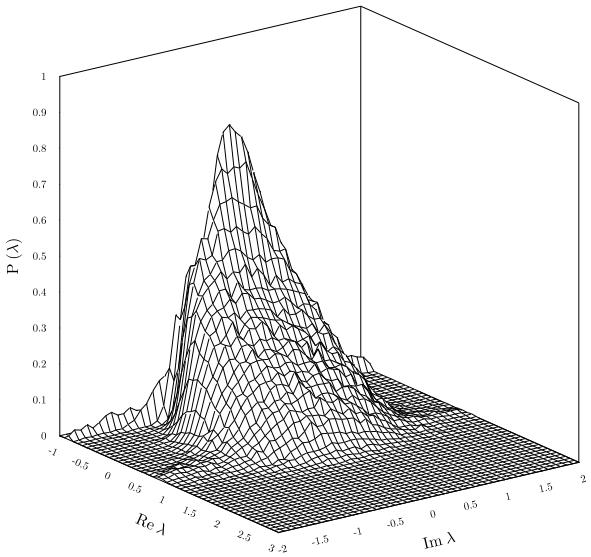

Fig. 1.6 Surface plot of the density of eigenvalues $P(\lambda)$ calculated for 1000 different distributions of $N = 100$ point-like scatterers placed randomly inside a sphere, with uniform density $n = 1$ scatterer per wavelength cubed. It shows clearly where the most weight of the $P(\lambda)$ distribution is located.

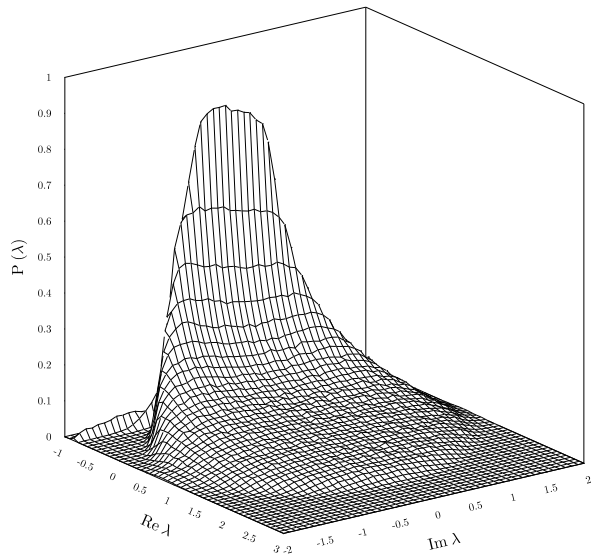

Fig. 1.7 Surface plot of the density of eigenvalues $P(\lambda)$ calculated for 500 different distributions of $N = 1000$ point-like scatterers placed randomly inside a sphere, with uniform density $n = 1$ scatterer per wavelength cubed. For increasing values of N, the probability distribution $P(\lambda)$ apparently moves towards the $\mathrm{Re}\lambda = -1$ axis and, simultaneously, its variance along the $\mathrm{Im}\lambda = \mathrm{const}$ axes decreases.

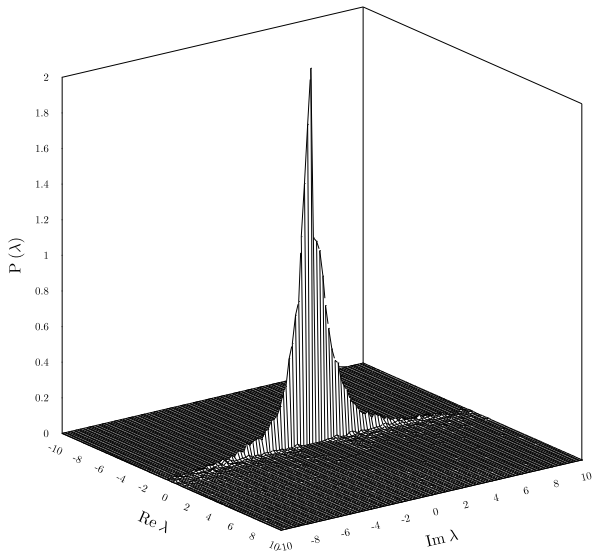

Fig. 1.8 Surface plot of the density of eigenvalues $P(\lambda)$ calculated for 100 different distributions of $N = 100$ point-like one-dimensional scatterers placed randomly with uniform density $n = 1$ scatterer per wavelength.

$\mathrm{Im}\lambda = -\cot\phi$. In this case the corresponding eigenvector $\vec{\mathcal{E}}'(\vec{r}_a)$ of the $\hat{G}$ matrix is a nonzero solution of the system of linear equations (1.38) for the incoming wave $\vec{\mathcal{E}}^{(0)}(\vec{r}_a)$ equal to zero. Thus, as shown in Sec. 1.4, a localized wave exists.

In three dimensions, proofs of self-averaging are rare and in most cases quantities are not self averaging [52]. For waves propagating in one dimensional random systems (meaning that two out of three dimensions are translationally invariant and only the third is random) self-averaging can be demonstrated mathematically. For one-dimensional systems it was shown that for "almost any" energy or frequency an eigenfunction decays exponentially in space for "almost any" realization of the disorder [53, 54]. This fact is also unambiguously confirmed within one-dimensional version of our model. In Fig. 1.8 we present an one-dimensional counterpart of Figs. 1.6 and 1.7. It is easily seen from inspection of these figures that Eq. (1.49) is satisfied also for systems consisting of one-dimensional point-like scatterers. Moreover, this mathematical property of random Green matrices seems to be fulfilled also in 2D free-space case [38] and in the case of a 2D system with nontrivial boundary conditions [55] and thus appears to be truly universal.

1.9 ANDERSON LOCALIZATION

Electronic states in solids are usually either extended, by analogy with the Bloch picture for crystalline media, or are localized around *isolated* spatial regions such as surfaces and impurities. However, in the case of a sufficiently disordered system a countable set of discrete energies corresponding to localized states becomes dense in some finite interval. But, physically speaking, it is impossible to distinguish between the allowed energies which may be arbitrarily close to each other and the spectrum is always a coarse-grained object. Therefore an entire continuous band of spatially localized electronic states appears. Anderson localization occurs when this happens [56]. Similarly, it is reasonable to expect, that in the case of infinite and random collection of dielectric particles there can exist a band of localized electromagnetic waves corresponding to a region of frequencies ω. This analogy allows us to elaborate a physical interpretation of the results obtained with the point-scatterer model used.

Let us now apply our model to a system of identical dielectric spheres with given radiuses R and dielectric constants ϵ located randomly with uniform physical density η. In this case the parameter ϕ from Eq. (1.33) remains a function of the frequency, i.e., $\phi = \phi(\omega)$. It follows from Eq. (1.49), for almost any random distribution of the scatterers $\vec{r}_a$ (except maybe for a few special ones with measure zero) an infinite number of eigenvalues λ of the $\hat{G}$ matrix satisfies the condition

$$\mathrm{Re}\lambda_j(\omega) = -1 \tag{1.50}$$

(note that we added an index j which labels the localized waves). As pointed out before, this occurs not only for $n = 1$ but for a whole range of n and therefore, for fixed physical density ρ, for a range of frequencies ω. Therefore at real values of frequency ω_j determined by the equation

$$\mathrm{Im}\lambda_j(\omega_j) = -\cot\phi(\omega_j) \tag{1.51}$$

these eigenvalues are solutions of Eq. (1.41). Thus the corresponding eigenvectors $\vec{\mathcal{E}}'_j(\vec{r}_a)$ of the $\hat{G}$ matrix describe localized states which exist at *discrete* frequencies ω_j. Note, that this result does not depend on the particular model of the scatterer used.

Let us observe that the $\hat{G}$ matrix from Eq. (1.39) is a *traceless* matrix, i.e., $\sum_i \lambda_i = 0$. This means that it is impossible for all eigenvalues to fulfill the localization condition Eq. (1.50). The inspection of Figs. 1.2 and 1.3 suggest that these eigenvalues may be a first approximations to very broad resonances responsible for enhanced coherent backscattering from a random medium. This so called weak localization is usually considered as a precursor of the strong localization (Anderson localization). The property $\sum_i \lambda_i = 0$ serves also as a good test for accuracy of our numerical procedures.

It seems reasonable to expect that the function f from Eq. (1.49) has compact support:

$$f(\mathrm{Im}\lambda) = 0 \quad \text{for} \quad |\mathrm{Im}\lambda| > \mathrm{Im}\lambda_{\mathrm{cr}} \tag{1.52}$$

(the values of $\mathrm{Im}\lambda_{\mathrm{cr}}$ should be regarded as functions of ω). According to Eq. (1.51) this means that localized waves of frequency ω can exist only if

$$|\phi(\omega)| \geq \phi_{\mathrm{cr}}(\omega), \tag{1.53}$$

where

$$\cot \phi_{\mathrm{cr}}(\omega) = \mathrm{Im}\lambda_{\mathrm{cr}}(\omega). \tag{1.54}$$

We see from Eqs. (1.35) and (1.53) that the total scattering cross section of individual particles σ must exceed some critical value $\sigma_{\mathrm{cr}} = \sigma(\phi_{\mathrm{cr}})$ before localization will take place in the limit $N \to \infty$. This fact is in perfect agreement with the scaling theory of localization [18]: in 3D random media a certain critical degree of disorder is needed for localization.

Moreover, our preliminary calculations indicate that the value of $k^2\sigma_{\mathrm{cr}}$ may decrease with n but *slower* than n^{-2}. Using the Rayleigh expression for the total scattering cross-section σ of a dielectric sphere with radius R and dielectric constant ϵ [25]:

$$k^2\sigma = \frac{8}{3\pi}(kR)^6 \left|\frac{\epsilon - 1}{\epsilon + 1}\right|^2, \tag{1.55}$$

we conclude that in the long-wave limit the system of dielectric spheres distributed with constant density $\eta = k^3 n/(2\pi)^3$ will be out of the localization regime. On the other hand in the limit of small wavelengths, the the propagation of light is ruled by the laws of geometrical optics and the point-scatterer approximation we use, becomes invalid. Therefore our results seem to agree with the common believe (see, e.g., [14, 15]), that in three-dimensional media localization of light is possible only in a certain frequency window:

$$\omega_{\min} \leq \omega \leq \omega_{\max}. \tag{1.56}$$

In the limit $N \to \infty$ a countable set of discrete frequencies ω_j corresponding to localized waves becomes dense in this finite interval given by Eq. (1.56). Thus an entire *band* of spatially localized waves appears in the limit of an infinite medium. Physically speaking this means that different realizations of sufficiently large *disordered* system are practically (i.e., by a transmission experiment) indistinguishable from each other. Similarly, as pointed out by Anderson, in a sufficiently disordered solid an entire band of spatially localized electronic states can be formed [1, 24].

By analogy with the electron case, the phenomenon of Anderson localization of electromagnetic waves should manifest itself as an inhibition of the

transmission in a spatially random dielectric medium. We have already some numerical evidence that it is actually true in the case of two-dimensional system consisting of randomly distributed dielectric cylinders [55]. The validity of this connection in the considered three-dimensional model would attribute sound interpretation and clear physical meaning to the continuous region of frequencies corresponding to localized waves. We expect that for each point ω from this region, incident waves with frequency ω will be totally reflected by almost any random distribution of the spheres $\vec{r}_a$ with scattering properties $\phi(\omega)$.

1.10 BRIEF SUMMARY

We have presented a quite realistic point-scatterer model describing scattering of electromagnetic waves by a disordered dielectric medium. Its relative simplicity allowed us to discover some new features of the Anderson localization of electromagnetic waves in 3D dielectric media without using any averaging procedures. Within our theoretical approach one can easily see how localization "sets in" for increasing size of the system. Very striking universal properties of the spectra of random matrices describing the scattering from a collection of randomly distributed point-like scatterers have been observed. Self-averaging of the real parts of the eigenvalues emerging in the limit of an infinite medium has been discovered numerically. For the first time (to our knowledge) the appearance of the band of localized electromagnetic waves in 3D was demonstrated. Connection between this phenomenon and a dramatic inhibition of the propagation of electromagnetic waves in a spatially random dielectric medium has been sketched. It can be understood as a counterpart of Anderson localization in solid state physics.

REFERENCES

1. P. W. Anderson. Absence of diffusion in certain random lattices. *Phys. Rev.*, 109:1492, 1958.

2. M. Kaveh. What to expect from similarities between the Schrödinger and Maxwell equations. In van Haeringen and Lenstra [57], page 21.

3. S. John. Electromagnetic absorption in a disordered medium near a photon mobility edge. *Phys. Rev. Lett.*, 53:2169, 1984.

4. P. W. Anderson. The question of classical localization. A theory of white paint? *Phil. Mag. B*, 52:505, 1985.

5. S. John. Strong localization of photons in certain disordered dielectric superlattices. *Phys. Rev. Lett.*, 58:2486, 1987.

6. C. M. Soukoulis, editor. *Photonic Band Gaps and Localization*, New York, 1993. NATO ASI Series, Plenum.

7. E. Akkermans, P. E. Wolf, and R. Maynard. Coherent backscattering of light by disordered media: Analysis of the peak line shape. *Phys. Rev. Lett.*, 56:1471, 1986.

8. M. J. Stephen and G. Cwillich. Rayleigh scattering and weak localization: Effects of polarization. *Phys. Rev. B*, 34:7564, 1986.

9. F. C. MacKintosh and S. John. Coherent backscattering of light in the presence of time-reversal-noninvariant and parity-nonconserving media. *Phys. Rev. B*, 37:1884, 1988.

10. Y. Kuga and A. Ishimaru. Retroreflectance from a dense distribution of spherical particles. *J. Opt. Soc. Am. A*, 1:831, 1984.

11. M. P. van Albada and A. Lagendijk. Observation of weak localization of light in a random medium. *Phys. Rev. Lett.*, 55:2692, 1985.

12. P.-E. Wolf and G. Maret. Weak localization and coherent backscattering of photons in disordered media. *Phys. Rev. Lett.*, 55:2696, 1985.

13. S. John. Localization and absorption of waves in a weakly dissipative disordered medium. *Phys. Rev. B*, 31:304, 1985.

14. S. John. Photon localization: the inhibition of electromagnetism in certain dielectrics. In van Haeringen and Lenstra [57], page 105.

15. S. John. Localization of light. *Physics Today*, 44(5):32, 1991.

16. A. Ishimaru. *Wave Propagaton and Scattering in Random Media.* Academic, New York, 1978.

17. A. Kerker. *The Scattering of Light and Other Electromagnetic Radiation.* Academic, New York, 1969.

18. E. Abrahams, P. W. Anderson, D. C. Licciardello, and T. V. Ramakrishnan. Scaling theory of localization: Absence of quantum diffusion in two dimensions. *Phys. Rev. Lett.*, 42:673, 1979.

19. D. S. Wiersma, P. B.olini, A. Lagendijk, and R. Righini. Localization of light in a disordered media. *Nature*, 390:671, 1997.

20. A. Z. Genack and N. Garcia. Observation of photon localization in a three-dimensional disordered system. *Phys. Rev. Lett.*, 66:2064, 1991.

21. W. Götze. A theory for the conductivity of a fermion gas moving in a strong three-dimensional random potential. *J. Phys. C*, 12:1279, 1979.

22. W. Götze. *Phil. Mag. B*, 43:219, 1981.

23. D. Vollhardt and P. Wölfle. Diagramatic, self-consistent treatment of the Anderson localization problem in $d \leq 2$ dimensions. *Phys. Rev. B*, 22:4666, 1980.

24. P. W. Anderson. Localized moments and localized states. *Rev. Mod. Phys.*, 50:191, 1978.

25. J. D. Jackson. *Classical Electrodynamics*. John Wiley and Sons Inc, New York, 1962.

26. M. Born and E. Wolf. *Principles of Optics*. Pergamon Press, Oxford-London, 1965.

27. B. A. Lippmann and J. Schwinger. Variational principles for scattering processes. *Phys. Rev.*, 79:469, 1950.

28. M. P. van Albada, B. A. van Tiggelen, A. Lagendijk, and A. Tip. Speed of propagation of classical waves in strongly scattering media. *Phys. Rev. Lett.*, 66:3132, 1991.

29. Yu. N. Barabanenkov and V. D. Ozrin. Problem of light diffusion in strongly scattering media. *Phys. Rev. Lett.*, 69:1364, 1992.

30. B. A. van Tiggelen, A. Lagendijk, M. P. van Albada, and A. Tip. Speed of light in random media. *Phys. Rev. B*, 45:12233, 1992.

31. J. Kroha, C. M. Sokoulis, and P. Wölfle. Localization of classical waves in a random medium: A self-consistent theory. *Phys. Rev. B*, 47:11093, 1993.

32. B. A. van Tiggelen and E. Kogan. Analogies between light and electrons: Density of states and Friedel's identity. *Phys. Rev. A*, 49:708, 1994.

33. C. M. Soukoulis, S. Datta, and E. N. Economou. Propagation of classical waves in random media. *Phys. Rev. B*, 49:3800, 1994.

34. P. A. Lee and A. D. Stone. Universal conductance fluctuations in metals. *Phys. Rev. Lett.*, 55:1622, 1985.

35. M. B. van der Mark, M. P. van Albada, and A. Lagendijk. Light scattering in strongly scattering media: Multiple scattering and weak localization. *Phys. Rev. B*, 37:3575, 1988.

36. B. A. van Tiggelen, A. Lagendijk, and A. Tip. Multiple-scattering effects for the propagation of light in 3d slabs. *J. Phys. C*, 2(37):7653, 1990.

37. M. Rusek and A. Orłowski. Analytical approach to localization of electromagnetic waves in two-dimensional random media. *Phys. Rev. E*, 51(4):R2763, 1995.

38. M. Rusek, A. Orłowski, and J. Mostowski. Band of localized electromagnetic waves in random arrays of dielectric cylinders. *Phys. Rev. E*, 56(4):4892, 1997.

39. M. Rusek, A. Orłowski, and J. Mostowski. Localization of light in three-dimensional random dielectric media. *Phys. Rev. E*, 53(4):4122, 1996.

40. M. Rusek and A. Orłowski. Example of self-averaging in three dimensions: Anderson localization of electromagnetic waves in random distributions of pointlike scatterers. *Phys. Rev. E*, 56(5B):6090, 1997.

41. E. M. Purcell and C. R. Pennypacker. Scattering and absorption of light by nonspherical dielectric grains. *Astrophys. J.*, 186(186):705, 1973.

42. C. F. Bohren and D. R. Huffman. *Absorption and Scattering of Light by Small Particles*. Wiley, New York, 1983.

43. B. T. Draine and P. J. Flatau. Discrete-dipole approximation for scattering calculations. *J. Opt. Soc. Am. A*, 11:1491, 1994.

44. B. A. van Tiggelen. PhD thesis, University of Amsterdam, Amsterdam, 1992.

45. T. M. Nieuwenhuizen, A. Lagendijk, and B. A. van Tiggelen. Resonant point scatterers in multiple scattering of classical waves. *Phys. Lett. A*, 169:191, 1992.

46. E. J. Heller. Quantum proximity resonances. *Phys. Rev. Lett.*, 77(20):4122, 1996.

47. J. S. Hersch and E. J. Heller. Observation of proximity resonances in a parallel-plate waveguide. *Phys. Rev. Lett.*, 81(15):3059, 1998.

48. I. Tolstoy. Superresonant systems of scatterers. *J. Acoust. Soc. Am.*, 80(1):282, 1986.

49. I. Tolstoy and A. Tolstoy. Superresonant systems of scatterers. ii. *J. Acoust. Soc. Am.*, 83(6):2086, 1988.

50. C. Feuillade. Scattering from collective modes of air bubbles in water and the physical mechanism of superresonances. *J. Acoust. Soc. Am.*, 98(2):1178, 1995.

51. V. A. Markel. Scattering of light from two interacting spherical particles. *Journal of Modern Optics*, 39:853, 1992.

52. A. Lagendijk and B. A. van Tiggelen. Resonat multiple scattering of light. *Phys. Rep.*, 270(3):143, 1996.

53. H. Furstenberg. Noncommuting random matrices. *Trans. Am. Math. Soc*, 108:377, 1963.

54. F. Deylon, H. Kunz, and B. Souillard. One-dimensional wave equations in disordered media. *J. Phys. A*, 16:25, 1983.

55. M. Rusek and A. Orłowski. Anderson localization of electromagnetic waves in confined dielectric media. *Phys. Rev. E*, 59(3):3655, 1999.

56. B. Souillard. Waves and electrons in inhomogeneous media. In Jean Souletie, Jean Vannimenus, and Raymond Stora, editors, *Chance and Matter*, number XLVI in Les Houches, page 305. North-Holland, Amsterdam, 1987.

57. W. van Haeringen and D. Lenstra, editors. *Analogies in Optics and Micro Electronics*. Kluwer, Dordrecht, 1990.